Economical Operation of Microgrid With Various Devices Via Distributed Optimization

Zaiyue Yang, *Member, IEEE*, Rui Wu, Jinfeng Yang, Keyu Long, and Pengcheng You, *Student Member, IEEE*

***Abstract*—This paper aims at minimizing economical cost of a microgrid by jointly scheduling various devices, e.g., appliances, batteries, thermal generators, and wind turbines. To properly model the system, the characteristics of all devices is fully investigated; in particular, the chance constraint is introduced to capture the randomness of power generation of wind turbines. Then, this problem is formulated as a large-scale mixed-integer program with coupling constraints. In order to solve this problem efficiently, it is decoupled via dual decomposition into a set of subproblems to be solved distributedly on each appliance, battery, and generator. While the scheduling of generator is well studied in literature, this paper specially proposes an efficient method for appliance scheduling, and then employs Benders' decomposition for battery scheduling. The performance of the proposed approach is verified by numerical simulations.**

***Index Terms*—Benders' decomposition, distributed implementation, dual decomposition, microgrid, optimal operation.**

NOMENCLATURE

Parameters of Appliance Model

$\mathcal{H} \triangleq \{1, \ldots, H\}$	Time slots of a day (equally divided).
p_0^h	Fixed load of nonshiftable appliances.
$\mathcal{A}$	Set of shiftable appliances.
a	Shiftable appliance belongs to $\mathcal{A}$.
$\mathcal{H}_a \triangleq [h_a^{\text{beg}}, h_a^{\text{end}}]$	Working interval for shiftable appliance.
$\boldsymbol{p}_a \triangleq [p_a^1, \ldots, p_a^H]$	Corresponding energy consumption vector of appliance a.
$p_a^{\min}$, $p_a^{\max}$	Minimum and maximum energy consumption of appliance a.
$\bar{p}_a^h$	Target energy consumption.
D_a	Total power appliance a needed to accomplish a task.

Parameters of Battery Model

B	Battery set.
b	Battery belongs to B.
u_c^h, u_d^h	Charging and discharging signal.
$p_{b,c}^h$, $p_{b,d}^h$	Charging and discharging rate of battery b.
$p_{b,c}^{\max}$, $p_{b,d}^{\max}$	Maximum charging and discharging rate of battery b.
e_b^h	Remaining energy of battery b at slot h.
$e_b^{\min}$, $e_b^{\max}$	Energy lower bound and upper bound of battery b.
e_b^0	Initial energy of battery b.
η_b^c, η_b^d	Charging and discharging efficiencies of battery b.
r_b	Cost per unit of battery charging/ discharging power.

Parameters of Thermal Generator Model

$\mathcal{G}$	Generator set.
u_g^h	On/off state of generator g.
p_g^h	Output of generator g at slot h.
$T_{g,\text{on}}^h$, $T_{g,\text{off}}^h$	Cumulative uptime and off-time at slot h.
$T_{g,\text{up}}$, $T_{g,\text{down}}$	Minimum turn-on and shutdowntime of generator g.
$p_g^{\min}$, $p_g^{\max}$	Output bounds of thermal generators.
$\epsilon_{g,1}$, $\epsilon_{g,2}$, $\epsilon_{g,3}$	Cost coefficients of generator g.
R_g^h	Start-up cost of generator g at slot h.
$R_{g,\text{hot}}$, $R_{g,\text{cold}}$	Hot start-up cost and cold start-up cost.
$T_{g,\text{cold}}$	Cooling time of generator g.

Parameters of Wind Turbine Model

p_w^h	Power generation of wind turbine at time slot h.
v	Wind velocity.
v_{in}, v_{out}	Cut-in and cut-out wind speed.
v_r	Rated wind speed.
p_{rate}	Rated power.
c, κ	Scale parameter and shape parameter of Weibull distribution.

Parameters of Problem Formulation

s_h	Power purchased from power grid at slot h.

Manuscript received September 27, 2014; revised May 15, 2015 and July 20, 2015; accepted September 10, 2015. Date of publication October 9, 2015; date of current version February 17, 2016. This work was supported in part by the National Natural Science Foundation of China under Grant 61371159, in part by the National High Technology Research and Development Program of China (863 Program) under Grant 2012AA041709, and in part by the Zhejiang International Collaboration Project under Grant 2013C24008. Paper no. TSG-00960-2014. *(Corresponding author: Zaiyue Yang.)*

The authors are with the State Key Laboratory of Industrial Control Technology, Zhejiang University, Hangzhou 310027, China (e-mail: yangzy@zju.edu.cn; wurui20wurui@163.com; jfyang90@gmail.com; longkywell@gmail.com; pcyou@zju.edu.cn).

Color versions of one or more of the figures in this paper are available online at http://ieeexplore.ieee.org.

Digital Object Identifier 10.1109/TSG.2015.2479260

$s^{\max}$	Maximum power purchased from main grid.
φ^h	Tolerable output of wind turbine.
ρ	Given tolerability.
c^h	Known electricity price at slot h.
$\boldsymbol{\lambda}$,$\boldsymbol{\mu}$	Lagrangian multipliers.
τ_a, ψ_a^h, $\xi_a^h \geq 0$	Karush–Kuhn–Tucker (KKT) operators.
$\sigma_{b,c}^h(n)$, $\sigma_{b,d}^h(n)$	Lagrange multipliers.
$\theta_{b,1}^h(n)$, $\theta_{b,2}^h(n)$	Lagrange multipliers.

I. Introduction

WITH THE ever increasing energy demand, the power grid is experiencing significant changes. Owing to high energy utilization and reliability, distributed generation (DG) attracts great attention. However, direct connection between DG and power grid causes high connection cost and generation uncertainty. The microgrid provides an alternative, which combines DG, energy storage devices, load, and control devices together and supplies electricity at consumer side [1]. Meanwhile, microgrid is able to respond quickly to the power grid and satisfy various demands of consumers.

As the key feature of microgrid, optimal operation methodologies have been extensively investigated, which can be classified into demand side management (DSM) and supply side management (SSM). References [2]–[12] focus on the DSM issues of microgrid. Price schemes (real-time price [4] and time-of-use price [5]) are introduced to induce consumers to shift load from peak periods. References [6]–[8] employ batteries as temporary storage on account of their extra flexibility. On the other hand, the SSM issues also attract great attentions. The power of microgrid mainly consists of three parts: 1) purchased power from power grid; 2) generated power from thermal generators in microgrid; and 3) renewable energy sources. Reasonable unit commitment (UC) [13], [14] facilitates the microgrid to dynamically select purchasing power or generating power according to electricity prices and operating cost of generators. When renewable energy sources are considered, a variety of models have been proposed to describe the randomness of renewable power generation, especially for wind turbines [15]–[17].

Due to kinds of constraints imposed in microgrid, such as supply-demand balance constraint, capacity constraint, binary constraint on energy storage, and the optimization problem of economic operation cannot be directly tackled. Thus, dual decomposition and Benders' decomposition are often used to tackle those constraints, which also decompose the original problem into a series of subproblems (SPs). Dual decomposition is used in [18] and [19] to handle the balance and capacity constraints. Benders' decomposition is also widely used in power systems to coordinate the optimization of various objectives [20]–[22]. For example, Su *et al.* [23] developed a decomposition scheme to solve the mixed integer nonlinear programming (MINP) problem formulated in microgrid. Similar technique has been developed to solve the optimal operation problem in microgrid which contains photovoltaics and a wind turbine [24].

Despite these results, previous studies still lack comprehensive investigations of microgrid operation from both supply and demand sides. To this end, this paper fully considers various devices in microgrid, such as appliances, batteries, thermal generators and wind turbines, and comprehensively study the joint scheduling problem of such a microgrid. The main difference between microgrid and distribution network lies in the fact that in microgrid the distributed energy resources are directly connected and operate in a coordinated way, either in grid-connected or islanded mode.

Meanwhile, as the microgrid often consists of a large number of devices, the computational efficiency becomes a major concern of algorithm design, and some previous algorithms [10]–[12] cannot be directly applied to this paper due to computational inefficiency. In this paper, a fully distributed approach is proposed to tackle the joint scheduling problem of microgrid.

The main contributions are listed below.

1) The joint scheduling of energy generation, consumption and storage is considered in this paper. In particular, the chance constraint is introduced to capture the randomness of power generation of wind turbines.
2) As the joint scheduling problem is formulated as a large-scale MINP with coupling constraints, a distributed framework is developed to solve this problem in parallel via dual decomposition.
3) To further speed up the efficiency under this parallel scheme, a novel efficient method is designed to schedule the appliance, besides using Benders' decomposition to schedule the battery.

In summary, this paper presents a computational efficient method to solve the scheduling problem of a microgrid for economic operation, provided that the future load and electricity price are available. However, in reality the future load and electricity price cannot be forecasted accurately. To mitigate this gap, a two-level framework combining online updating and static scheduling can be utilized. At the upper level, the change of both price and load will be updated in real time; then at the lower level, those quantities will be taken as constants and the static scheduling problem will be solved by the proposed approach. As the proposed approach is very efficient, it can fit in this framework very well, even when the price and load are updated frequently to eliminate the effect of uncertainty. As the two-level framework is easy to understand and implement, in this paper we shall focus on the efficient solution to the static scheduling problem.

In order to highlight the algorithmic contributions, we simplify the physical structure of microgrid and only present a conceptual block diagram, as to be shown in Fig. 2. With this block diagram, the most important feature of a microgrid, i.e., the supply-demand balance, can be taken into full consideration. Consequently, further scheduling of the usage of various devices can be performed. Of course, taking the physical structure into consideration will certainly make this problem more realistic and challenging, which we shall work on in the future on the basis of current results.

This paper is organized as below. In Section II, the features of each type of devices are analyzed. Based on the

system model of microgrid, the economical operation problem is formulated and further decomposed into a set of SPs in Section III. Section IV proposes novel algorithms to solve the SPs for appliance and battery, followed by simulations in Section V.

II. System Model

In this paper, we consider a microgrid containing several types of devices, such as, appliances, batteries, generator sets and wind turbines. A block diagram is given in Fig. 2. Each device is equipped with a local controller (LC) for computation and execution, and all LCs are coordinated by a central controller (CC) via local area network communications [25]. For simplicity, transmitting electricity from batteries back to the grid is not considered here. Meanwhile, let a day be equally divided into time slots denoted by $\mathcal{H} \triangleq \{1, \ldots, H\}$.

A. Appliance Model

The appliances can be classified into two types: 1) non-shiftable appliances with fixed load p_0^h like refrigerator and 2) shiftable appliances [6] like dishwasher, which is denoted by $\mathcal{A}$. Clearly, only shiftable appliances can be scheduled.

Let $\mathcal{H}_a \triangleq [h_a^{\text{beg}}, h_a^{\text{end}}]$ represent the working interval for shiftable appliance $a \in \mathcal{A}$, and $\boldsymbol{p}_a \triangleq [p_a^1, \ldots, p_a^H]$ be the corresponding energy consumption vector of appliance a, where non-negative p_a^h is the energy consumption of appliance a at slot h. Due to the working interval limits, p_a^h is bounded as

$$\begin{cases} p_a^{\min} \le p_a^h \le p_a^{\max}, & h \in \mathcal{H}_a \\ p_a^h = 0, & h \notin \mathcal{H}_a \end{cases} \tag{1}$$

where $p_a^{\min}$ and $p_a^{\max}$ are the minimum and maximum energy consumption of appliance a. Usually, the total consumption of appliance a should reach a given amount D_a to accomplish a task, which can be formulated as a constraint, that is

$$\sum_{h \in \mathcal{H}} p_a^h = D_a, \forall a \in \mathcal{A}. \tag{2}$$

Meanwhile, the scheduling of appliance may cause user dissatisfaction, which is often formulated as a convex function [26]

$$V_a^h\left(p_a^h\right) = o_a^h\left(p_a^h - \bar{p}_a^h\right)^2$$

where $\bar{p}_a^h$ and o_a^h are the target energy consumption and trade-off factors, which can be obtained from historical data. The similar idea has been widely used in [18] and [26].

B. Battery Model

Let $\mathcal{B}$ denote the battery set with multiple batteries, which can store energy when charging and supply energy to appliances when discharging. Note that all batteries in the set should have the same charging and discharging states at slot h, because interchange of energy among batteries will not bring any benefit but cause battery degradation. Denote the state of battery set as $u_c^h, u_d^h \in \{0, 1\}$, where $u_c^h = 1$ or $u_d^h = 1$ implies charging or discharging. Since charging and discharging cannot take place simultaneously, we have

$$u_c^h + u_d^h \le 1, \forall h \in \mathcal{H}. \tag{3}$$

Meanwhile, the charging rate $p_{b,c}^h$ and discharging rate $p_{b,d}^h$ of battery b are limited by the following constraints:

$$\begin{cases} p_{b,c}^h \ge 0, p_{b,d}^h \ge 0 & \text{(4a)} \\ p_{b,c}^h \le u_c^h p_{b,c}^{\max}, p_{b,d}^h \le u_d^h p_{b,d}^{\max} & \text{(4b)} \end{cases}$$

where $p_{b,c}^{\max}$ and $p_{b,d}^{\max}$ are the maximum charging and discharging rates, respectively. The dynamics of remaining energy e_b^h of battery b at slot h are obtained as follows:

$$e_b^h = e_b^0 + \sum_{t=1}^{h} \left(\eta_b^c p_{b,c}^t - \frac{p_{b,d}^t}{\eta_b^d} \right)$$

where e_b^0, η_b^c, and η_b^d are the initial energy, charging, and discharging efficiencies of battery b. With consideration of the energy constraints of battery, we have

$$e_b^{\min} \le e_b^h \le e_b^{\max}. \tag{5}$$

Both charging and discharging actions will cause battery degradation, which can be counted as financial cost

$$\sum_{h \in \mathcal{H}} r_b \left(p_{b,d}^h + p_{b,c}^h \right) \tag{6}$$

where r_b stands for the cost per unit of battery charging/discharging power, with the unit of cent/kW [27].

C. Thermal Generator Model

The ability to operate in isolated state is the main feature of microgrid due to DGs. In this paper, generator sets and the wind turbines are discussed as the representatives of DGs.

Let $\mathcal{G}$ be the generator set. For generator g, define integer variable u_g^h as the on/off state, with $u_g^h = 1$ for "on" and $u_g^h = 0$ for "off." Denote $T_{g,\text{on}}^h$, $T_{g,\text{off}}^h$, $T_{g,\text{up}}$, and $T_{g,\text{down}}$ as the cumulative uptime and off-time at slot h and the minimum turn-on time and shutdown time of generator g. Due to the physical constraints that state shifting can only take place after a fixed time interval, the state variables of two adjacent slot should follow the rule [28]:

$$\begin{cases} \left(T_{g,\text{on}}^{h-1} - T_{g,\text{up}} \right) \left(u_g^h - u_g^{h-1} \right) \ge 0 & \text{(7a)} \\ \left(T_{g,\text{off}}^{h-1} - T_{g,\text{down}} \right) \left(u_g^{h-1} - u_g^h \right) \ge 0. & \text{(7b)} \end{cases}$$

The output power of generator g at slot h is always limited by power bounds $p_g^{\min}$ and $p_g^{\max}$, that is

$$p_g^{\min} \le p_g^h \le p_g^{\max}. \tag{8}$$

Meanwhile, the operating cost $f_g(p_g^h)$ of generator g is formulated as follows [28]:

$$f_g\left(p_g^h\right) = \epsilon_{g,1} + \epsilon_{g,2} p_g^h + \epsilon_{g,3} \left(p_g^h\right)^2 \tag{9}$$

where $\epsilon_{g,1}$, $\epsilon_{g,2}$, and $\epsilon_{g,3}$ are the cost coefficients of generator g. The start-up cost R_g^h of generator g at slot h is relative to its operating state

$$R_g^h = \begin{cases} R_{g,\text{hot}} & T_{g,\text{off}}^h \le T_{g,\text{down}} + T_{g,\text{cold}} \\ R_{g,\text{cold}} & T_{g,\text{off}}^h > T_{g,\text{down}} + T_{g,\text{cold}} \end{cases} \tag{10}$$

where $R_{g,\text{hot}}$, $R_{g,\text{cold}}$, and $T_{g,\text{cold}}$ are the hot start-up cost, cold start-up cost, and cooling time of generator g, respectively. Finally, the total cost of generator set is obtained

$$\sum_{g\in\mathcal{G}}\sum_{h\in\mathcal{H}}\left[f_g\left(p_g^h\right) + R_g^h\left(1-u_g^{h-1}\right)\right]u_g^h. \tag{11}$$

D. Probability Model of Wind Turbine

The power generation of wind turbines is influenced by numerous factors, such as wind velocity, efficiency, and so on. For simplicity, the relationship between the power generation of wind turbine p_w and wind velocity v is expressed by the piecewise function [29]

$$p_w(v) = \begin{cases} 0, & v < v_{\text{in}} \text{ or } v \ge v_{\text{out}} \\ \dfrac{(v-v_{\text{in}})p_{\text{rate}}}{v_r - v_{\text{in}}}, & v_{\text{in}} \le v < v_r \\ p_{\text{rate}}, & v_r \le v < v_{\text{out}} \end{cases} \tag{12}$$

where v_{in}, v_{out}, v_r, and p_{rate} are the cut-in wind speed, cut-out wind speed, rated wind speed, and rated power, respectively. Usually, p_{rate} stands for the maximum output of wind turbine.

Prior research [30] has shown that the short-term wind speed profile at a given location closely follows the Weibull Distribution over time, similar idea can be found in [31]–[33]. Thus the wind speed in short-term is considered to obey the Weibull distribution in this paper, which is

$$F_v(v) = 1 - \exp\left[-\left(\frac{v}{c}\right)^{\kappa}\right] \tag{13}$$

where positive variables c and κ are the scale parameter and shape parameter, respectively.

Based on the characteristic of the wind power (12) and the pdf of wind speed (13), the pdf of wind power is obtained

$$F(p_w) = \begin{cases} 0, & p_w < 0 \\ 1 - \exp\left\{-\left[\dfrac{v_{\text{in}} + (v_r - v_{\text{in}})\dfrac{p_w}{p_{\text{rate}}}}{c}\right]^{\kappa}\right\} & \\ \quad + \exp\left[-\left(\dfrac{v_{\text{out}}}{c}\right)^{\kappa}\right], & 0 \le p_w < p_{\text{rate}} \\ 1, & p_w \ge p_{\text{rate}}. \end{cases} \tag{14}$$

III. Problem Formulation and Decomposition

A. Economical Operation of Microgrid

Denote s_h as the power purchased from power grid at slot h, which is limited by the cable constraint $s^{\max}$

$$-s^{\max} \le s^h \le s^{\max}. \tag{15}$$

Positive (negative) s^h implies buying (selling) energy from (to) the main grid. Usually, it is expected that the supply equals the demand in microgrid at any slot. Due to the wind uncertainty, chance constraint is considered to handle the situation where demand exceeds supply. It is tolerant that the occurrence probability $\Pr(p_w^h \le \varphi^h)$ is not greater than a given tolerability ρ, where

$$\varphi^h = \sum_{a\in\mathcal{A}} p_a^h + p_0^h + \sum_{b\in\mathcal{B}} p_{b,c}^h - \sum_{g\in\mathcal{G}} u_g^h p_g^h - \sum_{b\in\mathcal{B}} p_{b,d}^h. \tag{16}$$

Hence, the chance constraint is formulated as $\Pr(p_w^h \le \varphi^h) = \rho$. With the wind power pdf in (14), we obtain

$$\Pr\left(p_w^h \le \varphi^h\right) = 1 - \exp\left\{-\left[\frac{v_{\text{in}} + (v_r - v_{\text{in}})\frac{p_w}{p_{\text{rate}}}}{c}\right]^{\kappa}\right\} + \exp\left[-\left(\frac{v_{\text{out}}}{c}\right)^{\kappa}\right] = \rho. \tag{17}$$

With another constraint $\rho \ge \Pr(p_w^h = 0)$, the chance constraint is transformed as

$$\sum_{g\in\mathcal{G}} u_g^h p_g^h + s^h + \sum_{b\in\mathcal{B}} p_{b,d}^h + \omega^h p_{\text{rate}} = \sum_{a\in\mathcal{A}} p_a^h + p_0^h + \sum_{b\in\mathcal{B}} p_{b,c}^h \tag{18}$$

where

$$\omega^h = \frac{c^h}{(v_r - v_{\text{in}})}\left|\ln\left\{\exp\left[-\left(\frac{v_{\text{out}}}{c}\right)^{\kappa^h}\right] - \rho + 1\right\}\right|^{\frac{1}{\kappa^h}} - \frac{v_{\text{in}}}{(v_r - v_{\text{in}})}. \tag{19}$$

The economical operation of microgrid aims at reducing the level of user dissatisfaction, battery losses, the cost of purchasing power, and operating generation set under all kinds of constraints. Meanwhile due to the uncertainty of wind, this paper does not take wind power generation as a control variable, but only as a constraint variable. Therefore, it is not included in the objective function. In conclusion, this problem is formulated as a large-scale mixed-integer program as follows.

Primal Problem:

$$\begin{aligned} \min_{p,u,s}\ \mathcal{P} = & \sum_{h\in\mathcal{H}}\sum_{g\in\mathcal{G}}\left[f_g\left(p_g^h\right) + R_g^h\left(1-u_g^{h-1}\right)\right]u_g^h + \sum_{h\in\mathcal{H}} c^h s^h \\ & + \sum_{h\in\mathcal{H}}\sum_{a\in\mathcal{A}} V_a^h\left(p_a^h\right) + \sum_{h\in\mathcal{H}}\sum_{b\in\mathcal{B}} r_b^h\left(p_{b,c}^h + p_{b,d}^h\right) \\ \text{s.t.}\quad & (1),\ (2),\ (3),\ (4a),\ (4b),\ (5),\ (7a),\ (7b),\ (8),\ (15),\ (18) \end{aligned} \tag{20}$$

where c^h is the known electricity price at slot h.

B. Dual Decomposition

As (20) is hard to handle due to integer variables and coupling constraints, dual decomposition is applied to decouple it into several SPs of different types of devices.

To deal with the constraint (18) which couples all devices, the Lagrangian multipliers $\boldsymbol{\lambda} \triangleq [\lambda^1, \ldots, \lambda^H]$ and $\boldsymbol{\mu} \triangleq [\mu^1, \ldots, \mu^H]$ are defined corresponding to $s^h \le s^{\max}$ and $s^h \ge 0$, respectively. Therefore, the Lagrangian

formula of (20) is derived

$$L(p,u,\lambda,\mu)=\sum_{g\in\mathcal{G}}\sum_{h\in\mathcal{H}}\left[f_g\left(p_g^h\right)+R_g^h\left(1-u_g^{u-1}\right)-\alpha^h p_g^h\right]u_g^h+\sum_{b\in\mathcal{B}}\sum_{h\in\mathcal{H}}\left[\left(\alpha^h+r_b\right)p_{b,c}^h-\left(\alpha^h-r_b\right)p_{b,d}^h\right]+\sum_{a\in\mathcal{A}}\sum_{h\in\mathcal{H}}\left[\alpha^h p_a^h+V_a^h\left(p_a^h\right)\right]+\urcorner \tag{21}$$

where $\alpha^h \triangleq c^h+\lambda^h-\mu^h$ and $\urcorner \triangleq \sum_{h\in\mathcal{H}}\alpha^h\left(p_0^h-\omega^h p_{\text{rate}}\right)-\sum_{h\in\mathcal{H}}\lambda^h s^{\max}$ which is independent of p_a, p_b, u_b, p_g, and u_g. The primal problem (20) is equivalent to the following equation:

$$\mathcal{P}^*=\min_{p,u}\max_{\lambda,\mu}L(p,u,\lambda,\mu).$$

Next, the dual problem of (20) is considered as

Dual Problem:

$$\begin{aligned}\mathcal{D}^*&=\max_{\lambda,\mu:\lambda,\mu\geq 0}\min_{p,u,s}L\left(p,u_g,\lambda,\mu\right)\\&=\max_{\lambda,\mu:\lambda,\mu\geq 0}\sum_{a\in\mathcal{A}}L_1+\max_{\lambda,\mu:\lambda,\mu\geq 0}L_2\\&\quad+\max_{\lambda,\mu:\lambda,\mu\geq 0}\sum_{g\in\mathcal{G}}L_3+\max_{\lambda,\mu:\lambda,\mu\geq 0}\urcorner.\end{aligned} \tag{22}$$

It is clear that the dual problem is composed of two level optimizations. The outer level is to maximize the dual function over λ and μ, while the inner level is divided into three SPs corresponding to appliances L_1, batteries L_2, and generators L_3, respectively as below.

Subproblems:

$$L_1=\min_{p_a}\sum_{h\in\mathcal{H}}\left[\alpha^h p_a^h+V_a^h\left(p_a^h\right)\right]\quad\text{s.t.}\quad(1),(2) \tag{23}$$

$$L_2=\min_{p_b,u_b}\sum_{b\in\mathcal{B}}\sum_{h\in\mathcal{H}}\left[\left(\alpha^h+r_b\right)p_{b,c}^h-\left(\alpha^h-r_b\right)p_{b,d}^h\right]\quad\text{s.t.}\quad(3),(4a),(4b),(5) \tag{24}$$

$$L_3=\sum_{h\in\mathcal{H}}L_3^h=\min_{p_g,u_g}\sum_{h\in\mathcal{H}}\left[f_g\left(p_g^h\right)+R_g^h\left(1-u_g^{u-1}\right)-\alpha^h p_g^h\right]u_g^h\quad\text{s.t.}\quad(7a),(7b),(8). \tag{25}$$

Note that there exists duality gap between primal problem (20) and dual problem (22) since the integer variables u_b and u_g lead to weak duality. For each feasible solution of $\mathcal{P}$, the corresponding $\mathcal{D}$ is the lower bound of $\mathcal{P}$ [34].

As the primal problem is convex, the subgradient method which guarantees the optimality of Lagrange multipliers is introduced to maximize the dual function over λ and μ. The updating rule of Lagrangian multipliers is

$$\begin{cases}\lambda^h(k+1)=\left\{\lambda^h(k)+\gamma_\lambda\nabla\mathcal{D}\left[\lambda^h(k)\right]\right\}^+\\ \mu^h(k+1)=\left\{\mu^h(k)+\gamma_\mu\nabla\mathcal{D}\left[\mu^h(k)\right]\right\}^+\end{cases} \tag{26}$$

where k and γ_λ, γ_μ are the iteration index and step sizes, respectively. $\nabla\mathcal{D}[\lambda^h(k)]$ and $\nabla\mathcal{D}[\mu^h(k)]$ are the subgradients of dual function with respect to $\lambda^h(k)$ and $\mu^h(k)$, which is relative to the solution of (23)–(25). Hence, the dual decomposition algorithm is obtained as Algorithm 1.

Algorithm 1 Dual Decomposition

1: Initialize iteration index $k=1$ and Lagrange multipliers $\lambda^h(k)$ and $\mu^h(k)$.
2: **repeat**
3: The central controller sends $\lambda^h(k)$, $\mu^h(k)$ to LCs of appliances, generators and batteries;
4: LCs of appliances, generators and batteries solve the subproblems (23)(24)(25) with $\lambda^h(k)$ and $\mu^h(k)$ to obtain $p_a^h(k)$, $p_{b,c}^h(k)$, $p_{b,d}^h(k)$, $p_g^h(k)$, $u_g^h(k)$.
5: The central controller updates $\lambda^h(k+1)$, $\mu^h(k+1)$ according to (26).
6: **until** k exceeds the maximum iteration number or $\mathcal{P}-\mathcal{D}$ is small enough.

IV. Subproblem Solution

Note that SP L_3 for the UC of a single generator has been well studied in literature, and it can be solved by either heuristic method [28] or dynamic programming [35]. Thus, the contributions in this section lie on the novel solutions to L_1 and L_2. Due to page limitation, only the sketches will be given.

A. Fast Method for Single Appliance Scheduling

Indeed, the scheduling of single appliance (23) is a convex problem that can be solved by many techniques. However, a more efficient algorithm is proposed for real-time scheduling of large-scale appliances.

Take appliance a as an example. The KKT conditions associated with the optimum of (23) is

$$\begin{cases}2o_a^h p_a^h+\alpha^h-\tau_a+\psi_a^h-\xi_a^h=0 & \text{(27a)}\\ \tau_a\left(D_a-\sum_{h\in\mathcal{H}}p_a^h\right)=0 & \text{(27b)}\\ \psi_a^h\left(p_a^h-p_a^{\max}\right)=0 & \text{(27c)}\\ \xi_a^h\left(p_a^{\min}-p_a^h\right)=0 & \text{(27d)}\end{cases}$$

where $\tau_a, \psi_a^h, \xi_a^h \geq 0$ are KKT operators. Taking τ_a as a variable and solving above linear equations yield

$$\begin{cases}p_a^h(\tau_a)=\max\left\{\min\left\{\dfrac{\tau_a-\alpha_a}{2o_a^h},p_a^{\max}\right\},p_a^{\min}\right\} & \text{(28a)}\\ \psi_a^h(\tau_a)=\max\left\{\tau_a-\alpha_a-2o_a^h p_a^{\max},0\right\} & \text{(28b)}\\ \xi_a^h(\tau_a)=\max\left\{2o_a^h p_a^{\min}+\alpha_a-\tau_a,0\right\}. & \text{(28c)}\end{cases}$$

The detailed derivation of above equations is straightforward but tedious, thus it is omitted for simplicity.

Obviously, (28a) implies that once the optimal τ_a^* is determined, the optimal p_a^h is also found. Thus, the question becomes to solve τ_a^*, which should also obey (27b). For holding (27b), we have two possible cases: 1) $\tau_a^*=0$ or 2)

$$\tilde{D}_a\left(\tau_a^*\right)\triangleq\sum_{h\in\mathcal{H}}p_a^h\left(\tau_a^*\right)=D_a. \tag{29}$$

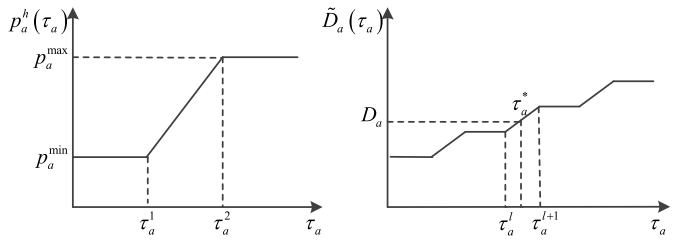

Fig. 1. Profile of $p_a^h(\tau_a)$ and $\tilde{D}_a(\tau_a)$ are both step function, which allow us to solve the problem by Algorithm 2.

Algorithm 2 Single Appliance Scheduling

if $\tilde{D}_a(0) \geq D_a$ **then**
  $\tau_a^* = 0$.
else
  Initialize $l = 1$, $r = 2H$.
  while $r - l > 1$ **do**
    $m = \lfloor (l + r)/2 \rfloor$ and $d = \sum_{h \in H} p_a^h(\tau_a^m)$.
    if $d = D_a$ **then**
      $\tau_a^* = \tau_a^m$.
    else if $d < D_a$ **then**
      $l = m$.
    else
      $r = m$.
    end if
  end while
  $\tau_a^* = \tau_a^l + \left(\tau_a^{l+1} - \tau_a^1\right) \frac{D_a - \tilde{D}_a(\tau_a^l)}{\tilde{D}_a(\tau_a^{l+1}) - \tilde{D}_a(\tau_a^l)}$.
end if
$p_a^{h*} = p_a^h(\tau_a^*)$.

Note that $p_a^h(\tau_a)$ is a piecewise linear and monotonic increasing function of τ_a, so is $\tilde{D}_a(\tau_a)$. That is, $\tilde{D}_a(x) \geq \tilde{D}_a(0)$ for $x \geq 0$. Therefore, we can conclude that: 1) if $\tilde{D}_a(0) \geq D_a$, only the first case is possible, i.e., $\tau_a^* = 0$ and 2) if $\tilde{D}_a(0) < D_a$, only the second case (29) is possible.

Due to the piecewise linear and monotonic increasing properties of $\tilde{D}_a(\tau_a)$, a simple and efficient method is proposed to solve (29). The basic idea is presented below. $p_a^h(\tau_a)$ is a piecewise function with two breaking points $\tau_a^1 = 2o_a^h p_a^{\min} + \alpha_a$ and $\tau_a^2 = 2o_a^h p_a^{\max} + \alpha_a$. According to (28a), $p_a^h(\tau_a)$ consists of three segments, i.e., $p_a^h = p_a^{\min}$ when $0 \leq \tau_a \leq \tau_a^1$, $p_a^h = (\tau_a - \alpha_a/2o_a^h)$ when $0 \leq \tau_a \leq \tau_a^1$, and $p_a^h = p_a^{\max}$ when $\tau_a \geq \tau_a^2$. Because $\tilde{D}_a(\tau_a)$ is the summation of number H of $p_a^h(\tau_a)$, it is also piecewise linear and monotonic increasing, and has totally $2H$ breaking points. Fig. 1 illustrates the profiles of $p_a^h(\tau_a)$ and $\tilde{D}_a(\tau_a)$.

From Fig. 1(b), it is clear that solving (29) only needs two steps. First, sort $2H$ breaking points in ascending order and find an appropriate pair of breaking points (via binary search here), e.g., τ_a^l and τ_a^{l+1}, such that $\tilde{D}_a(\tau_a^l) \leq D_a \leq \tilde{D}_a(\tau_a^{l+l})$. Clearly, τ_a^* lies between τ_a^l and τ_a^{l+1}. Then, direct compute τ_a^* via interpolation with the slope of this segment. When τ_a^* is obtained, (28a) readily gives p_a^h. The details are summarized in Algorithm 2.

B. Battery Scheduling Based on Benders' Decomposition

As a mixed integer linear program (MILP), SP L_2 of battery scheduling contains integer and continuous variables and cannot be directly solved by conventional methods. Benders' decomposition [36] is an effective method to solve MILP, based on which an iterative algorithm is proposed in this section.

Clearly, the constraints of (24) can be classified into three types: 1) (3) contains only integer variables; 2) (4a) and (5) contain continuous variables; and 3) (4b) contains both integer and continuous variables. Then, (24) can be rewritten as

$$\begin{aligned} \min_{u_b, p_b} \mathcal{Z} &\triangleq \sum_{b \in \mathcal{B}} z_b \triangleq \sum_{b \in \mathcal{B}} \sum_{h \in \mathcal{H}} \left[\left(\alpha^h + r_b\right) p_{b,c}^h - \left(\alpha^h - r_b\right) p_{b,d}^h \right] \\ \text{s.t.} \quad & (3) \quad \text{integer constraint} \\ & (4a)(5) \quad \text{continuous constraints} \\ & (4b) \quad \text{integer and continuous constraints.} \end{aligned} \tag{30}$$

The core of Benders' decomposition lies in splitting (30) into a master problem (MP) and an SP, separately optimizing integer and continuous variables, as below.

Master Problem:

$$\begin{aligned} \mathcal{Z}_{\text{lower}} = \min_{u_b} \ & \mathcal{Z} \\ \text{s.t.} \quad & (3) \\ & \text{feasibility constraints} \\ & \text{infeasibility constraints.} \end{aligned} \tag{31}$$

Subproblem:

$$\begin{aligned} \mathcal{Z}_{\text{upper}} = \min_{p_b} \ & \mathcal{Z} \\ \text{s.t.} \quad & (4a)\ (5) \\ & (4b) \text{ given } u_b. \end{aligned} \tag{32}$$

The objective functions of (30) and (31) are identical, but (30) neglects the constraints with continuous variables p_b; thus, MP produces the lower bound of $\mathcal{Z}$. Meanwhile, both feasibility and infeasibility constraints are integer ones, which are iteratively updated based on the solution of SP and help find more suitable integer variables, as to be detailed later.

Once given integer variables u_b, MILP retreats to SP (32) that is an easy-solved linear program (LP). However, as the given u_b may not be the optimal one u_b^*, SP only produces the upper bound of $\mathcal{Z}$. Clearly, $\mathcal{Z}_{\text{lower}} \leq \mathcal{Z}^* \leq \mathcal{Z}_{\text{upper}}$. Therefore, $\mathcal{Z}^*$ can be found by performing iterations between MP and SP, such that $\mathcal{Z}_{\text{lower}}$ and $\mathcal{Z}_{\text{upper}}$ converge together. The iteration begins with any feasible solution $u_b(0)$, and is detailed below.

1) Solving SP at Iteration n: Given $u_b(n)$, the coupling constraints among batteries are naturally decoupled, and SP for battery set is decomposed into B primal SPs for each battery $b \in \mathcal{B}$ as follows.

Primal SP:

$$\begin{aligned} \min_{p_b(n)} \ & z_b \\ \text{s.t.} \quad & (4a)(5) \\ & (4b) \text{ given } u_b(n). \end{aligned} \tag{33}$$

Introduce Lagrange multipliers $\sigma^h_{b,c}(n)$, $\sigma^h_{b,d}(n)$, $\theta^h_{b,1}(n)$, and $\theta^h_{b,2}(n)$ to constraints (4b) and (5) at slot h. Therefore, the Lagrangian form of (33) is derived as follows:

$$\begin{aligned}
&\mathcal{L}\left[\boldsymbol{p}(n), \boldsymbol{\sigma}_{b,c}(n), \boldsymbol{\sigma}_{b,d}(n), \boldsymbol{\theta}_{b,1}(n), \boldsymbol{\theta}_{b,2}(n)\right] \\
&= \sum_{h\in\mathcal{H}} \left\{ \alpha^h + r_b + \sigma^h_{b,c}(n) + \eta^c_b \sum_{t=h}^{H} \left[\theta^t_{b,1}(n) - \theta^t_{b,2}(n)\right] \right\} p^h_{b,c} \\
&\quad + \sum_{h\in\mathcal{H}} \left\{ -\alpha^h + r_b + \sigma^h_{b,d}(n) - \frac{1}{\eta^c_d} \sum_{t=h}^{H} \left[\theta^t_{b,1}(n) - \theta^t_{b,2}(n)\right] \right\} p^h_{b,d} \\
&\quad - \sum_{h\in\mathcal{H}} \left[u^h_c(n) p^{\max}_{b,c} \sigma^h_{b,c}(n) + u^h_d(n) p^{\max}_{b,d} \sigma^h_{b,d}(n) \right] \\
&\quad + \sum_{h\in H} \left[\left(e^0_b - e^{\max}_b\right)\theta^h_{b,1}(n) + \left(e^{\min}_b - e^0_b\right)\theta^h_{b,2}(n) \right]. \qquad (34)
\end{aligned}$$

Due to the duality principle, every LP has an equivalent dual form, and the constraints and variables in primal problem correspond to the variables and constraints in dual problem. Thus in the dual form of (33), $\sigma^h_{b,c}(n)$, $\sigma^h_{b,d}(n)$, $\theta^h_{b,1}(n)$, and $\theta^h_{b,2}(n)$ turn into decision variables, while $p^h_{b,c}$ and $p^h_{b,d}$ become Lagrange multipliers. As presented below.

Dual SP:

$$\begin{aligned}
\max_{\substack{\boldsymbol{\sigma}_{b,c}(n), \boldsymbol{\sigma}_{b,d}(n), \\ \boldsymbol{\theta}_{b,1}(n), \boldsymbol{\theta}_{b,2}(n)}} \; y_b = &\sum_{h\in\mathcal{H}} \Big[-u^h_c(n) p^{\max}_{b,c} \sigma^h_{b,c}(n) \\
&\qquad - u^h_d(n) p^{\max}_{b,d} \sigma^h_{b,d}(n) \Big] \\
&+ \left(e^0_b - e^{\max}_b\right) \sum_{h\in\mathcal{H}} \theta^h_{b,1}(n) \\
&+ \left(e^{\min}_b - e^0_b\right) \sum_{h\in\mathcal{H}} \theta^h_{b,2}(n) \\
\text{s.t.} \quad \alpha^h + r_b + \sigma^h_{b,c}(n) + \eta^c_b &\sum_{t=h}^{H} \left[\theta^t_{b,1}(n) - \theta^t_{b,2}(n)\right] \geq 0 \\
- \alpha^h + r_b + \sigma^h_{b,d}(n) - &\frac{1}{\eta^c_d} \sum_{t=h}^{H} \left[\theta^t_{b,1}(n) - \theta^t_{b,2}(n)\right] \geq 0 \\
\sigma^h_{b,c}(n) \geq 0, \sigma^h_{b,d}(n) &\geq 0, \theta^h_{b,1}(n) \geq 0, \theta^h_{b,2}(n) \geq 0 \\
\forall h \in \mathcal{H}. \qquad (35)
\end{aligned}$$

Since strong duality holds for LP, the solution of (33) is equivalent to (35). That is, for $u_b(n)$ obtained from MP, we have

$$\min_{\boldsymbol{p}_b} z_b = \max_{\boldsymbol{\sigma}_{b,c}, \boldsymbol{\sigma}_{b,d}, \boldsymbol{\theta}_{b,1}, \boldsymbol{\theta}_{b,2}} y_b. \qquad (36)$$

2) Modifying and Solving MP at Iteration $n+1$: After solving all B dual SPs, one can obtain better integer variables $u^h_b(n+1)$ by adding new integer constraints to MP in iteration $n+1$. These new constraints are updated in three manners based on the solution of (35).

1) All B dual SPs (35) have bounded optimal solutions. In this case, the integer variables $u^h_b(n)$ given by MP are feasible but not optimal if $\mathcal{Z}_{\text{lower}}$ is less than $\mathcal{Z}_{\text{upper}}$. In order to make $\mathcal{Z}_{\text{lower}}$ converge to $\mathcal{Z}_{\text{upper}}$, we should "lift up" $\mathcal{Z}_{\text{lower}}$ by adding a new constraint to MP, as below.
   a) *Feasibility Constraint:*

$$\begin{aligned}
\mathcal{Z} \geq \mathcal{Z}_{\text{lower}}(i) &= \sum_{b\in\mathcal{B}} \min_{\boldsymbol{p}_b} z_b(i) = \sum_{b\in\mathcal{B}} \max_{\boldsymbol{\sigma}_{b,c}, \boldsymbol{\sigma}_{b,d}, \boldsymbol{\theta}_{b,1}, \boldsymbol{\theta}_{b,2}} y_b(i) \\
&= \sum_{b\in\mathcal{B}} \sum_{h\in\mathcal{H}} \left[-u^h_c(i) p^{\max}_{b,c} \sigma^h_{b,c}(i) - u^h_d(i) p^{\max}_{b,d} \sigma^h_{b,d}(i) \right] \\
&\quad + \left(e^0_b - e^{\max}_b\right) \sum_{b\in\mathcal{B}} \sum_{h\in\mathcal{H}} \theta^h_{b,1}(i) \\
&\quad + \left(e^{\min}_b - e^0_b\right) \sum_{b\in\mathcal{B}} \sum_{h\in\mathcal{H}} \theta^h_{b,2}(i) \qquad \forall i \in \mathcal{I} \quad (37)
\end{aligned}$$

   where $\mathcal{I}$ is the iteration set where all dual SPs are bounded optimal. Clearly, n should be incorporated into set $\mathcal{I}$, i.e., $\mathcal{I} = n \bigcup \mathcal{I}$. By this means, $u^h_b(n+1)$ will be improved because some feasible regions with poor solutions are cut out.
2) Any dual SP (35) owns unbounded optimal solution. This means that the integer variables $u^h_b(n)$ are infeasible for SPs and ought to be avoided in later iterations. Adding new infeasibility constraint helps cut such infeasible region out, which is as follows.
   a) *Infeasibility Constraint:*

$$\begin{aligned}
0 \geq &\sum_{h\in\mathcal{H}} \left[-u^h_c(j) p^{\max}_{b,c} \sigma^h_{b,c}(j) - u^h_d(j) p^{\max}_{b,d} \sigma^h_{b,d}(j) \right] \\
&+ \left(e^0_b - e^{\max}_b\right) \sum_{h\in\mathcal{H}} \theta^h_{b,1}(j) \\
&+ \left(e^{\min}_b - e^0_b\right) \sum_{h\in\mathcal{H}} \theta^h_{b,2}(j) \\
&\forall b \in \mathcal{B}, \forall j \in \mathcal{J} \qquad (38)
\end{aligned}$$

   where $\mathcal{J}$ is the iteration set where any dual SP is unbounded optimal. Then, set $\mathcal{J}$ is updated by $\mathcal{J} = n \bigcup \mathcal{J}$.
3) Any dual SP (35) is infeasible. Once this case occurs, the original problem has either an infeasible solution or unbounded solution. As the result, the scheduling problem has no physical solution.

Next, MP is solved by branch and bound method with fixed parameters $\boldsymbol{\sigma}_{b,c}(n)$, $\boldsymbol{\sigma}_{b,d}(n)$, $\boldsymbol{\theta}_{b,1}(n)$, and $\boldsymbol{\theta}_{b,2}(n)$.

In iterations of above steps, the feasible region gradually shrinks due to the added constraints based on the solutions of dual SPs. New $\mathcal{Z}_{\text{lower}}$ and $\mathcal{Z}_{\text{upper}}$ will converge to the optimal solution $\mathcal{Z}^*$. Denote ε as a small positive number. The iteration will not terminate until $|\mathcal{Z}_{\text{upper}} - \mathcal{Z}_{\text{lower}}| \leq \varepsilon$. The procedure of battery scheduling is summarized in Algorithm 3.

C. Distributed Implementation

An advantage of the proposed method is the distributed implementation, which can greatly reduce the computation time especially for microgrid with large amount of devices. Fig. 2 depicts the framework of distributed implementation.

The SPs of appliances (23), batteries (24), and generators (25) are solved by LCs. Since SPs (23) and (25) can

Algorithm 3 Battery Scheduling

1 htp

Initialization: $n = 0$, $\mathcal{I} = \emptyset$, $\mathcal{J} = \emptyset$, $\mathcal{Z}_{\text{upper}} = \infty$, $\mathcal{Z}_{\text{lower}} = -\infty$;
while n is less than the iteration limits **do**
  Solve MP (31) to obtain to obtain $u_b^h(n)$ and $\mathcal{Z}_{\text{lower}}$;
  if MP has feasible solution **then**
    if $\left|\mathcal{Z}_{\text{upper}} - \mathcal{Z}_{\text{lower}}\right| \le \varepsilon$ **then**
      $\boldsymbol{u}_b^* = \boldsymbol{u}_b(n)$.
    end if
  else if MP has unbounded solution **then**
    Choose $\boldsymbol{u}_b(n)$ from the domain of definition, $\mathcal{Z}_{\text{lower}} = -\infty$.
  else
    no feasible solution.
  end if
  for each battery $b \in \mathcal{B}$ **do**
    Solve dual SP (35) with $\boldsymbol{u}_b^h(n)$ to obtain $\boldsymbol{\sigma}_{b,c}(n)$, $\boldsymbol{\sigma}_{b,d}(n)$, $\boldsymbol{\theta}_{b,1}(n)$, $\boldsymbol{\theta}_{b,2}(n)$ and $z_b(n)$;
  end for
  if all dual SPs have feasible solution **then**
    $\mathcal{Z}_{\text{upper}} = \min\{\mathcal{Z}_{\text{upper}}, \sum_{b\in\mathcal{B}} z_b\}$, $\mathcal{I} = n \bigcup \mathcal{I}$.
  else if any dual SP has unbounded solution **then**
    $\mathcal{J} = n \bigcup \mathcal{J}$.
  else
    no feasible solution.
  end if
  $n = n + 1$.
end while

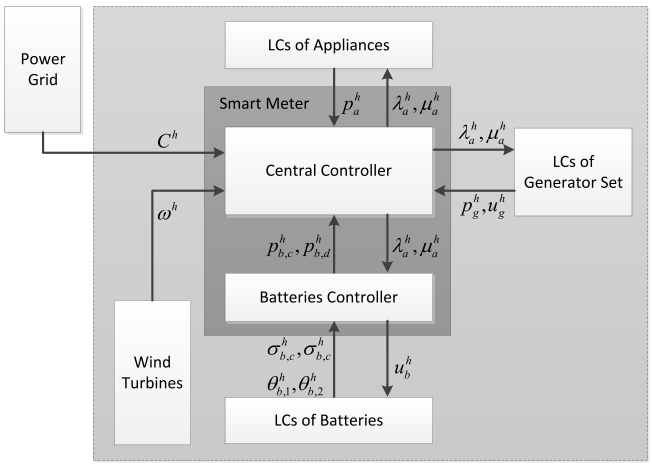

Fig. 2. Block diagram of microgrid and framework of distributed implementation.

be divided into scheduling of single device directly, each device owns an LC to obtain $\boldsymbol{p}_a$, $\boldsymbol{p}_g$, and $\boldsymbol{u}_g$ with given Lagrange multipliers $\boldsymbol{\lambda}$ and $\boldsymbol{\mu}$. Moreover, the coupling constraints between different batteries in SP (24) lead to an additional battery controller. The battery controller solves MP while the LCs of different batteries solves SPs.

The controller at smart meter which connects all devices, power grid and wind turbines together acts as the CC. Besides receiving the electricity prices and predicted information of wind turbines, it also gathers all the solutions of

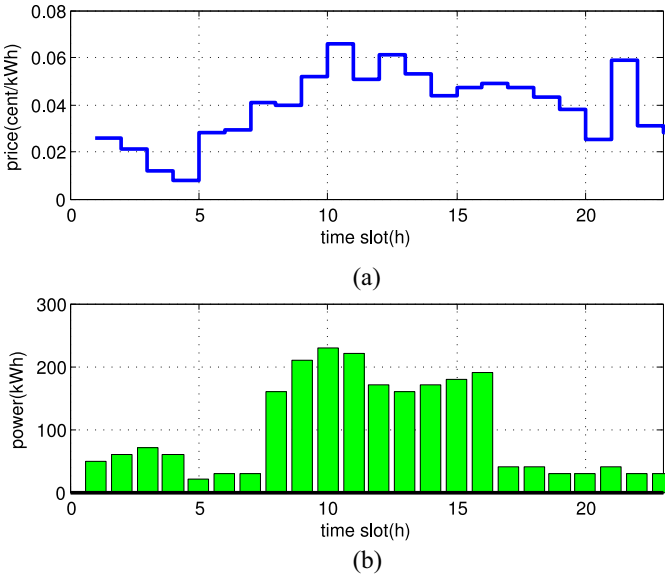

Fig. 3. (a) Electricity prices. (b) Nonshiftable load of appliances.

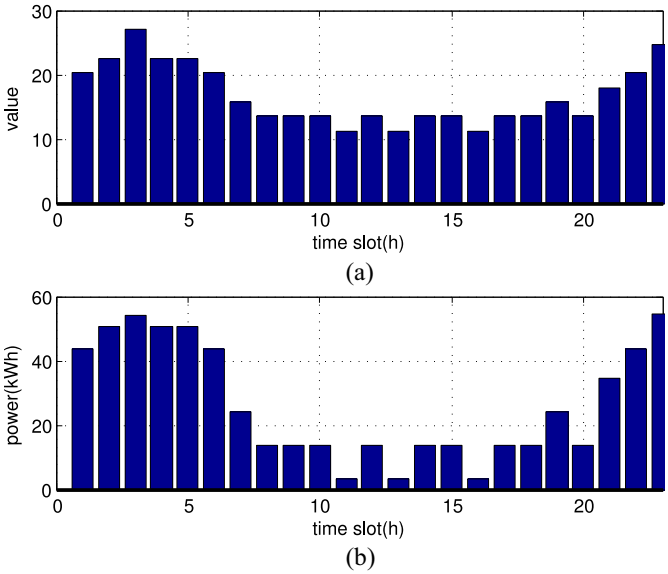

Fig. 4. Conservative power supply of wind turbines. (a) Change of scale parameter c. (b) Conservative output of the wind turbine.

SPs from LCs, battery controller and sends back the updated Lagrange multipliers to them. As the coordination signals, these multipliers gradually improve the local optimal solution into the global optimal solution.

V. Simulations and Results

In this section, the performance of microgrid scheme is presented. The horizon is taken as one day and then divided into $H = 24$ slots. Real prices on May 1, 2013 from ComEd [37] and the nonshiftable load of appliances depicted in Fig. 3 are utilized in the simulation.

Consider the scenario where the microgrid contains 100 appliances, five identical batteries, and one generator, whose parameters are displayed in Table I. Note that five different types of appliances are used in the simulation and the number of each type is random. The cut-in and cut-out wind

TABLE I
PARAMETERS OF APPLIANCES, BATTERIES, AND GENERATORS

Appliance							Battery			Generator		
Parameter	Unit	Type 1	Type 2	Type 3	Type 4	Type 5	Parameter	Unit	Value	Parameter	Unit	Value
h_a^{beg}	h	0	4	17	11	14	$e_b^{\min}$	kWh	1.776	$p_g^{\max}$	kW	200
h_a^{end}	h	23	11	21	15	19	$e_b^{\max}$	kWh	7.548	$p_g\min$	kW	50
D_a	kWh	18	16	8	8.75	5	e_b^0	kWh	1.776	$\epsilon_{g,1}$	$\$/h$	40
$p_a^{\max}$	kW	1	2.5	2	2	1.5	$p_{b,c}^{\max}$	kW	1.32	$\epsilon_{g,2}$	$\$/kWh$	16
o_a^h	-	0.1	0.2	0.1	0.1	0.2	$p_{b,d}^{\max}$	kW	1.77	$\epsilon_{g,3}$	$\$/kW^2h$	0.0015
							η_b^c	-	0.839	$T_{g,up}$	h	2
							η_b^d	-	0.764	$T_{g,down}$	h	2
										$T_{g,cold}$	h	0
										$R_{g,hot}$	$	700
										$R_{g,cold}$	$	1400

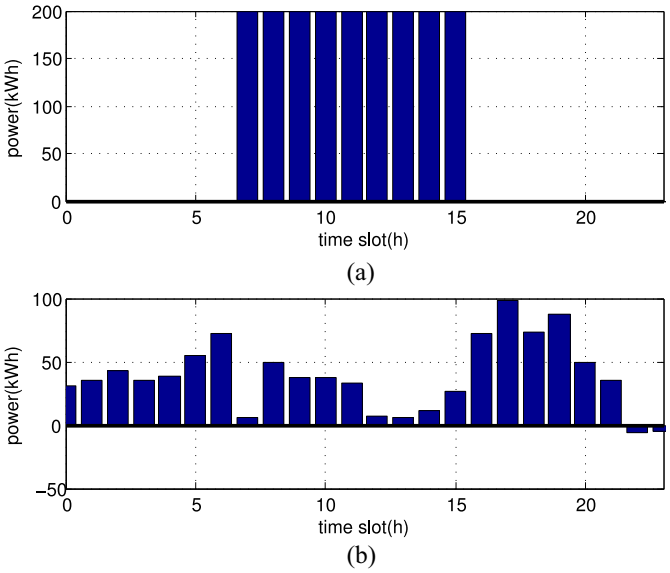

Fig. 5. Power of supply side. (a) Generating power of generator set. (b) Purchased power from grid.

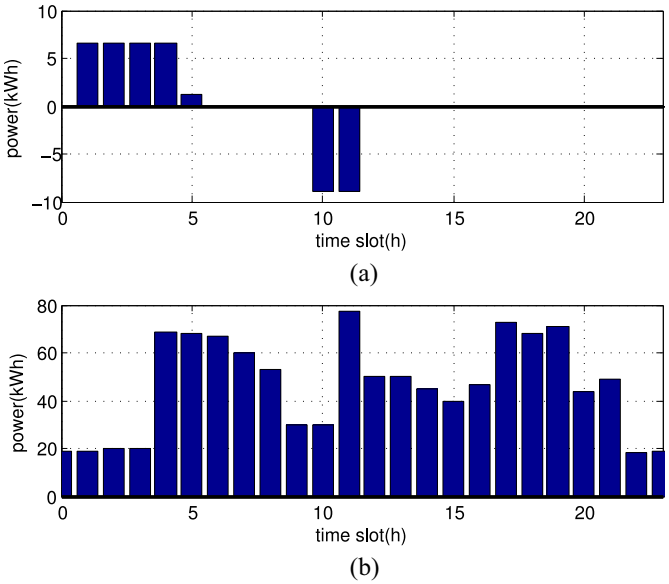

Fig. 6. Load of demand side. (a) Battery. (b) Smart appliance.

speed of wind turbine is set to be 5 and 45 m/s. Moreover, the rated wind speed and rated power are $v_r = 15$ m/s and $p_{\text{rate}} = 100$ kW. Let the shape parameter κ be 2, and the scale parameter c varies around 15 m/s as shown in Fig. 4(a). Fix the tolerability $\rho = 0.2$, then the corresponding conservative output of the wind turbine can be obtained in Fig. 4(b). The simulation is conducted with the iteration limit being 300.

Fig. 5 shows the optimal scheduling of supply side, including generator and power grid. It is obviously that under the shortage of wind power, the microgrid prefers purchasing electricity from power grid when the electricity prices are lower than the start-up cost and operating cost of generator. On the contrary, the microgrid is selling energy back to the main grid while the wind power is abundant. It takes generator as supplementary when the demand exceeds the supply of power grid, which occurs in the middle period of simulation.

The optimal operation of appliances and batteries are illustrated in Fig. 6. In Fig. 6(a), the batteries charge during the early morning when electricity prices are low and discharge when prices are high. The power profile of appliances in Fig. 6(b) indicates that the appliances avoid the peak-demand period in order to save the cost of microgrid.

The relationship between tolerability ρ, shape parameter κ, and the optimal cost of microgrid can be displayed in Fig. 7 by setting the scale parameter c at a constant 15 m/s. To some degree, tolerability ρ reflects the feasibility of the optimized strategy. Since (19) is a monotonically increasing function of ρ, a larger ρ indicates that wind turbines are likely to generate more power. On account of the fact that the power from wind turbines is free, the microgrid will save cost to a great extent. Therefore, the optimal cost obtained through proposed algorithms decreases as ρ increases while keeping other parameters unchanged. κ which indicates the probability distribution function of wind speed is also in negative relationship with the optimal cost.

Fig. 8 depicts the computation time of centralized and distributed implementation. The simulation is conducted using MATLAB R2011b on Windows 7. In this paper, "scale" means the multiple of the number of appliances, batteries and generators. Initially the scenario with 100 appliances, five identical batteries, and one generator is considered. So "ten times scale" means that the microgrid contains 1000 appliances, 50 batteries, and ten generators. As the

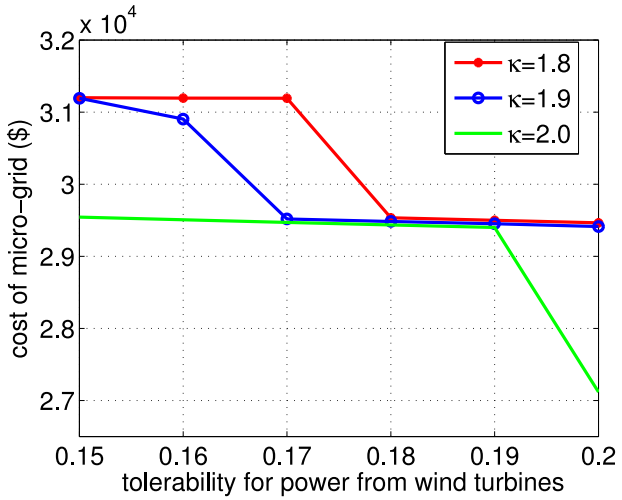

Fig. 7. Effect of tolerance on the scheduling cost.

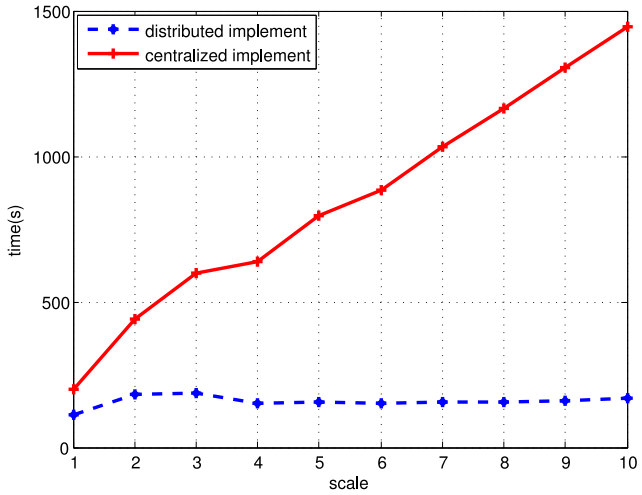

Fig. 8. Computation time of centralized and distributed implementation.

scale of micro-grid increases to ten times, the computation time of distributed implementation remains the same while that of centralized implementation grows linearly. The distributed implementation is especially suitable for large scale situation, since it dispatches the suboptimizations to LCs and saves the computation time greatly.

VI. Conclusion

In this paper, an approach improving the operation of large-scale of devices is developed to save the total cost of the microgrid. After introducing the chance constraint to represent the randomness of wind power, the scheduling problem is characterize into MINP, which is decomposed via Lagrange relaxation into three sets of SPs later, i.e., appliance scheduling, battery scheduling and generator scheduling. Since the generator scheduling is well studied in literature, in this paper an efficient method is proposed for appliance scheduling, and Benders' decomposition is employed for battery scheduling. Taking advantage of the distributed nature of proposed approach, parallel implementation is developed to reduce computation time in large-scale situation. Finally, simulation results validate the performance of our proposed algorithms.

A realistic concern of the proposed method is the time constant of a microgrid responding the power dispatch command. Knowing that the communication time and battery switching time are very small and can be neglected, the major factor of the time constant depends on thermal generator [38]. With the development of micro turbine like gas turbine, the time it takes to adjust the output can be limited in a minute [39]. Therefore, taking these aspects into consideration, we expect that a microgrid can respond the power dispatch command in a few minutes.

References

[1] J. Huang, C. Jiang, and R. Xu, "A review on distributed energy resources and microgrid," *Renew. Sustain. Energy Rev.*, vol. 12, no. 9, pp. 2472–2483, 2008.
[2] B. Chai, J. Chen, Z. Yang, and Y. Zhang, "Demand response management with multiple utility companies: A two-level game approach," *IEEE Trans. Smart Grid*, vol. 5, no. 2, pp. 722–731, Mar. 2014.
[3] A.-H. Mohsenian-Rad and A. Leon-Garcia, "Optimal residential load control with price prediction in real-time electricity pricing environments," *IEEE Trans. Smart Grid*, vol. 1, no. 2, pp. 120–133, Sep. 2010.
[4] S. N. Siddiqi and M. L. Baughman, "Reliability differentiated real-time pricing of electricity," *IEEE Trans. Power Syst.*, vol. 8, no. 2, pp. 548–554, May 1993.
[5] Y. Tang, H. Song, F. Hu, and Y. Zou, "Investigation on TOU pricing principles," in *Proc. IEEE/PES Transm. Distrib. Conf. Exhibit. Asia Pac.*, Dalian, China, 2005, pp. 1–9.
[6] A. Di Giorgio, L. Pimpinella, and F. Liberati, "A model predictive control approach to the load shifting problem in a household equipped with an energy storage unit," in *Proc. Mediterr. Conf. Control Autom.*, Barcelona, Spain, 2012, pp. 1491–1498.
[7] F. De Angelis *et al.*, "Optimal task and energy scheduling in dynamic residential scenarios," in *Proc. 9th Int. Symp. Neural Netw.*, Shenyang, China, 2012, pp. 650–658.
[8] A. Barbato *et al.*, "House energy demand optimization in single and multi-user scenarios," in *Proc. IEEE SmartGridComm*, Brussels, Belgium, 2011, pp. 345–350.
[9] R. Deng, Z. Yang, J. Chen, N. R. Asr, and M.-Y. Chow, "Residential energy consumption scheduling: A coupled-constraint game approach," *IEEE Trans. Smart Grid*, vol. 5, no. 3, pp. 1340–1350, May 2014.
[10] A. K. Pathak, S. Chatterji, and M. S. Narkhede, "Artificial intelligence based optimization algorithm for demand response management of residential load in smart grid," *Int. J. Eng. Innov. Technol.*, vol. 2, no. 4, pp. 136–141, 2012.
[11] J. M. Lujano-Rojas, C. Monteiro, R. Dufo-López, and J. L. Bernal-Agustín, "Optimum residential load management strategy for real time pricing (RTP) demand response programs," *Energy Pol.*, vol. 45, pp. 671–679, Jun. 2012.
[12] S. Nistor, J. Wu, M. Sooriyabandara, and J. Ekanayake, "Cost optimization of smart appliances," in *Proc. IEEE ISGT*, Manchester, U.K., 2011, pp. 1–5.
[13] T. Logenthiran and D. Srinivasan, "Short term generation scheduling of a microgrid," in *Proc. TENCON IEEE Region 10 Conf.*, Singapore, 2009, pp. 1–6.
[14] A. Khodaei, "Microgrid optimal scheduling with multi-period islanding constraints," *IEEE Trans. Power Syst.*, vol. 29, no. 3, pp. 1383–1392, May 2014.
[15] X. Liu and W. Xu, "Economic load dispatch constrained by wind power availability: A here-and-now approach," *IEEE Trans. Sustain. Energy*, vol. 1, no. 1, pp. 2–9, Apr. 2010.
[16] T. Malakar, S. K. Goswami, and A. K. Sinh, "Optimum scheduling of micro grid connected wind-pumped storage hydro plant in a frequency based pricing environment," *Int. J. Elect. Power Energy Syst.*, vol. 54, pp. 341–351, Jan. 2014.
[17] Y. Zhang, N. Gatsis, and G. B. Giannakis, "Robust energy management for microgrids with high-penetration renewables," *IEEE Trans. Sustain. Energy*, vol. 4, no. 4, pp. 944–953, Oct. 2013.
[18] R. Deng, Z. Yang, J. Chen, and M.-Y. Chow, "Load scheduling with price uncertainty and temporally-coupled constraints in smart grids," *IEEE Trans. Power Syst.*, vol. 29, no. 6, pp. 2823–2834, Nov. 2014.

[19] O. Ardakanian, S. Keshav, and C. Rosenberg, "Real-time distributed control for smart electric vehicle chargers: From a static to a dynamic study," *IEEE Trans. Smart Grid*, vol. 5, no. 5, pp. 2295–2305, Sep. 2014.
[20] M. Shahidehopour and Y. Fu, "Benders decomposition: Applying benders decomposition to power systems," *IEEE Power Energy Mag.*, vol. 3, no. 2, pp. 20–21, Mar./Apr. 2005.
[21] Z. Yang, K. Long, P. You, and M.-Y. Chow, "Joint scheduling of large-scale appliances and batteries via distributed mixed optimization," *IEEE Trans. Power Syst.*, vol. 30, no. 4, pp. 2031–2040, Jul. 2015.
[22] P. You and Z. Yang, "Efficient optimal scheduling of charging station with multiple electric vehicles via V2V," in *Proc. IEEE Int. Conf. Smart Grid Commun. (SmartGridComm)*, Venice, Italy, 2014, pp. 716–721.
[23] W. Su, J. Wang, and J. Roh, "Stochastic energy scheduling in microgrids with intermittent renewable energy resources," *IEEE Trans. Smart Grid*, vol. 5, no. 4, pp. 1876–1883, Jul. 2014.
[24] G. Kyriakarakos, A. I. Dounis, S. Rozakis, K. G. Arvanitis, and G. Papadakis, "Polygeneration microgrids: A viable solution in remote areas for supplying power, potable water and hydrogen as transportation fuel," *Appl. Energy*, vol. 88, no. 12, pp. 4517–4526, 2011.
[25] C.-P. Cheng, C.-W. Liu, and C.-C. Liu, "Unit commitment by Lagrangian relaxation and genetic algorithms," *IEEE Trans. Power Syst.*, vol. 15, no. 2, pp. 707–714, May 2000.
[26] L. Jiang and S. Low, "Multi-period optimal energy procurement and demand response in smart grid with uncertain supply," in *Proc. IEEE CDC-ECC*, Orlando, FL, USA, 2011, pp. 4348–4353.
[27] M. D. Hopkins, A. Pahwa, and T. Easton, "Intelligent dispatch for distributed renewable resources," *IEEE Trans. Smart Grid*, vol. 3, no. 2, pp. 1047–1054, Jun. 2012.
[28] T. Senjyu, K. Shimabukuro, K. Uezato, and T. Funabashi, "A fast technique for unit commitment problem by extended priority list," in *Proc. Power Eng. Soc. Gen. Meeting*, 2003, pp. 244–249.
[29] B. Beltran, T. Ahmed-Ali, and M. Benbouzid, "Sliding mode power control of variable-speed wind energy conversion systems," *IEEE Trans. Energy Convers.*, vol. 23, no. 2, pp. 551–558, Jun. 2008.
[30] M. R. Patel, *Wind and Solar Power Systems: Design, Analysis, and Operation*. Boca Raton, FL, USA: CRC Press, 2005.
[31] J. Hetzer, D. C. Yu, and K. Bhattarai, "An economic dispatch model incorporating wind power," *IEEE Trans. Energy Convers.*, vol. 23, no. 2, pp. 603–611, Jun. 2008.
[32] D. Villanueva, J. L. Pazos, and A. Feijoo, "Probabilistic load flow including wind power generation," *IEEE Trans. Power Syst.*, vol. 26, no. 3, pp. 1659–1667, Aug. 2011.
[33] A. M. Foley, P. G. Leahy, A. Marvuglia, and E. J. McKeogh, "Current methods and advances in forecasting of wind power generation," *Renew. Energy*, vol. 37, no. 1, pp. 1–8, 2012.
[34] S. P. Boyd and L. Vandenberghe, *Convex Optimization*. Cambridge, U.K.: Cambridge Univ. Press, 2004.
[35] R. Nieva, A. Inda, and I. Guillen, "Lagrangian reduction of search-range for large-scale unit commitment," *IEEE Trans. Power Syst.*, vol. 2, no. 2, pp. 465–473, May 1987.
[36] J. F. Benders, "Partitioning procedures for solving mixed-variables programming problems," *Numer. Math.*, vol. 4, no. 1, pp. 238–252, 1962.
[37] ComEd RRTP. (May 1, 2013). *ComEd Residential Real-Time Pricing Program*. [Online]. Available: https://rrtp.comed.com/
[38] J. M. Arroyo and A. J. Conejo, "Modeling of start-up and shut-down power trajectories of thermal units," *IEEE Trans. Power Syst.*, vol. 19, no. 3, pp. 1562–1568, Aug. 2004.
[39] P. Degobert, S. Kreuawan, and X. Guillaud, "Use of super capacitors to reduce the fast fluctuations of power of a hybrid system composed of photovoltaic and micro turbine," in *Proc. IEEE Int. Symp. Power Electron. Elect. Drives Autom. Motion (SPEEDAM)*, Taormina, Italy, 2006, pp. 1223–1227.

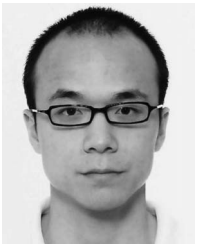

Zaiyue Yang (M'10) received the B.S. and M.S. degrees in control from the Department of Automation, University of Science and Technology of China, Hefei, China, in 2001 and 2004, respectively, and the Ph.D. degree in control from the Department of Mechanical Engineering, University of Hong Kong, Hong Kong, in 2008.

He was a Postdoctoral Fellow and a Research Associate with the Department of Applied Mathematics, Hong Kong Polytechnic University, Hong Kong. He joined Zhejiang University, Hangzhou, China, in 2010, where he is currently a Professor. His current research interests include smart grid, signal processing, and control theory.

Dr. Yang is an Associate Editor of the IEEE TRANSACTIONS ON INDUSTRIAL INFORMATICS.

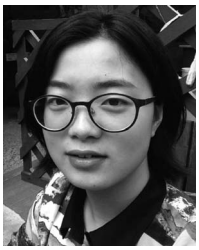

Rui Wu received the B.S. degree in manufacturing science and engineering from Sichuan University, Chengdu, China, in 2014. She is currently pursuing the Master's degree with the College of Control Science and Engineering, Zhejiang University, Hangzhou, China.

She is a Member of the Group of Networked Sensing and Control, State Key Laboratory of Industrial Control Technology, Zhejiang University. Her current research interests include optimization and data analysis in smart grid.

Jinfeng Yang received the B.S. degree in automation from Central South University, Changsha, China, in 2012, and the M.S. degree in control science and engineering from Zhejiang University, Hangzhou, China, in 2015.

She was a Member of the Group of Networked Sensing and Control, State Key Laboratory of Industrial Control Technology, Zhejiang University. Her current research interests include optimization and control of electric vehicles in smart grid.

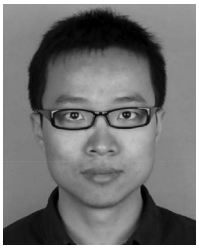

Keyu Long received the B.S. degree in automation from Xi'an Jiaotong University, Xi'an, China, in 2011, and the M.S. degree in control science and engineering from Zhejiang University, Hangzhou, China, in 2014.

He was a Member of the Group of Networked Sensing and Control, State Key Laboratory Industrial Control Technology, Zhejiang University. His current research interests include convex optimization, machine learning, and big data.

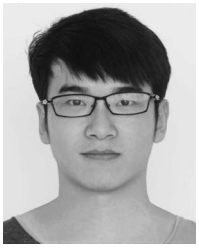

Pengcheng You (S'14) received the B.S. degree in electrical engineering from Zhejiang University, Hangzhou, China, in 2013, and the B.S. (Hons.) degree in engineering from Chu Kochen Honors College, Zhejiang University, where he is currently pursuing the Ph.D. degree with the College of Control Science and Engineering.

He is a Member of the Group of Networked Sensing and Control, State Key Laboratory of Industrial Control Technology, Zhejiang University. His current research interests include optimization and control in smart grid.